J. Membrane Biol. 123, 33–41 (1991)
0022263191001041

The Journal of
Membrane Biology

Ionic Basis of Methacholine-Induced Shrinkage of Dissociated Eccrine Clear Cells

Y. Suzuki, M. Ohtsuyama, G. Samman, F. Sato, and K. Sato
Marshall Dermatology Research Laboratories, Department of Dermatology, University of Iowa College of Medicine, Iowa City, Iowa 52242

Summary. The goal of the present study was to elucidate the ionic mechanisms by which cholinergic stimulation induces cell shrinkage in eccrine clear cells. Dissociated Rhesus monkey eccrine sweat clear cells were prepared by collagenase digestion of freshly isolated secretory coils and immobilized on a glass slide in a perfusion chamber at 30°C. The cell was visualized by light microscopy with differential interference contract (DIC) and was recorded with a video system (15,000× total magnification). The cell volume was calculated from the maximal cross section of the cell. Methacholine (MCh)-induced cell shrinkage, which was as much as 30% of resting cell volume, was dose dependent and pharmacologically specific. MCh-induced cell shrinkage was persistent in some cells but tended to partially wane with time in others. MCh-induced cell shrinkage was dependent on the chemical potential gradient for KCl, i.e., increasing [K] in the bath ($[K]_o$) from 5 to 120 mM caused MCh to induce cell swelling, whereas removing $[Cl]_o$ at 120 mM K partially restored the MCh-induced cell shrinkage. The interpolated null $[K]_o$ (medium [K] where the cell volume did not change by MCh) of 71 mM agreed with the predicted $[K]_{o,null}$. MCh-induced cell shrinkage was inhibited completely by 1 mM quinidine (K-channel blocker) and partially by 1 mM diphenylamine-2-carboxylic acid (DPC, a Cl-channel blocker), but not by 0.1 mM ouabain or 0.1 mM bumetanide, suggesting that MCh-induced cell shrinkage may be due to activation of both K and Cl channels with the resultant net KCl efflux down the chemical potential gradient. That Ca/calmodulin may be involved in cholinergic regulation of Cl and K channels is suggested because 10 μM ionomycin also induced cell shrinkage, MCh failed to induce cell shrinkage in a Ca-free medium after the endogenous Ca store was depleted, and (6-aminohexyl)-5-chloro-1-naphthalenesulfonamide (W-7, a putative inhibitor of calmodulin) also inhibited MCh-induced cell shrinkage in a reversible manner.

Key Words eccrine · sweat gland · cell volume · cholinergic · Ca · potassium · chloride · channels · quinidine

Introduction

We have recently reported that cholinergic stimulation of eccrine clear cells is associated with efflux of as much as 45% of the cytoplasmic K, an increase in cytoplasmic Na concentration ($[Na]_i$), cell volume decrease by as much as 28% (Saga & Sato, 1989; Takemura et al., 1991), and an increase in $[Ca]_i$ (Sato & Sato, 1988). The presence of both K and Cl channels has also been reported in freshly dissociated Rhesus secretory cells (Sato & Sato, 1989). Similar changes in cytoplasmic concentrations of monovalent ions and Ca as well as cell shrinkage have been reported to occur in mammalian exocrine acinar cells (Sasaki et al., 1983; Izutsu & Johnson, 1986; Foskett & Melvin, 1989), suggesting that the muscarinic regulation of ion transport among different exocrine acinar cells may be similar. Although cell volume regulation is an important cellular function in most epithelial and nonepithelial cells and has been subjected to extensive studies over the past two decades, most studies have addressed volume regulation on exposure to hyper- or hyposmotic environments (Chamberlin & Strange, 1989; Lewis & Donaldson, 1990). In other words, the occurrence of dramatic cell shrinkage during pharmacological stimulation in isotonic medium may be one of the characteristic features of exocrine acinar cells (Foskett & Melvin, 1989; Takemura et al., 1991). In our previous studies on eccrine clear cells, we used X-ray microanalysis and photographic methods. Unfortunately, these methods are rather cumbersome and not suitable for detailed studies on the mechanisms of cell shrinkage. In the present study, we employed a simple microscope video system for image analysis of eccrine clear cells in order to further examine the ionic mechanism of MCh-induced cell shrinkage using freshly dissociated Rhesus palm eccrine clear cells.

Materials and Methods

Isolation of Secretory Coils

Preparation of isolated Rhesus monkey palm sweat glands is essentially the same as described previously (Sato & Sato, 1981). Skin biopsy specimens, approximately 4 × 8 mm, were

repeatedly obtained from the palms of 15 monkeys tranquilized with a mixture of Ketalar (Parke-Davis) and Innovar (Janssen). In each monkey, skin biopsy was done at intervals no shorter than four weeks, and the areas of skin adjacent to previous biopsy sites were avoided. The excised tissue was blotted of blood, sliced into several pieces, and immediately washed in several changes of cold (about 10°C) modified Krebs-Ringer bicarbonate solution (KRB) containing (in mM): 125 NaCl, 5 KCl, 1.2 $MgSO_4$, 1.0 $CaCl_2$, 25 $NaHCO_3$, 1.2 NaH_2PO_4 (prepared by mixing one-tenth volume of each of the 10× stock solutions), 5.5 glucose, and 7% bovine serum albumin (BSA), at pH 7.48 and 5% CO_2/95% O_2. Single sweat glands were isolated under a stereomicroscope using sharp forceps in a dissection chamber kept at 14°C.

Preparation of Dissociated Secretory Coil Cells

Dissociated cells have been prepared according to Sato and Sato (1988) with modifications. Briefly, a minimum of 100 to 200 isolated whole sweat glands were first incubated with 0.75 mg/ml type I collagenase in Krebs bicarbonate buffer also containing 10 mM HEPES (HEPES-KRB, titrated to pH 7.48 with NaOH or KOH) for 15 min and then thoroughly washed in fresh (collagenase-free) HEPES-KREB. This brief collagenase digestion made the subsequent manual separation of the secretory coils from the ducts considerably easier. Isolated secretory coils were incubated in KRB containing 0.1 mM Ca, 0.75 mg/ml type I collagenase and 100 μg/ml DNAase I (all from Sigma) for 5 min at 37°C. The coils were incubated twice for 10 min in 500 μl of Ca- and Mg-free KRB containing 2 mM EGTA. A second enzyme digestion was performed for 30 to 60 min in KRB containing 0.1 mM Ca, 1.25 mg/ml collagenase or 0.125 mg/ml N-tosyl-L-phenylalanine chloromethyl ketone-treated trypsin (Sigma), penicillin (100 U/ml) and streptomycin (100 μg/ml) mixture, and 100 μg/ml DNAase. The cells were dispersed from the digested glands by repeatedly passing them through a sieve, which was a tungsten grid for electron microscopy (3-mm o.d., 100 mesh) epoxy glued to a disposable plastic pipette, the tip of which had been trimmed to 2-mm o.d. Dispersed cells were subsequently passed through a finer sieve (200–300 mesh) and centrifuged at 900× *g* for 2 min. The cells were then suspended in KRB containing 4% bovine albumin. The electron microscopy of the dispersed cells obtained in this way showed more than 60% secretory cells, less than 30% dark cells and about 10% myoepithelial cells. The mixed dispersed cells thus prepared were used for cell volume analysis because different cell types can be readily identified on the video screen (Figs. 1 and 2). More than 95% of these cells excluded Trypan blue.

Cell Volume Analysis by Light Microscopy with Differential Interference Contrast (DIC) and Video System

The construction of the superfusion chamber for cell volume analysis has been described previously (Takemura et al., 1991). Briefly, two strips of cover glass, 3.5 × 30 × 0.13 mm, were epoxy glued 3 mm apart in tandem on a 5 × 7 cm glass slide to create a groove 0.13 mm deep. The groove formed a slit when a polylysine-coated cover glass, 10 × 30 mm, with cells attached to its lower surface was mounted and sealed with silicone grease (Dow Corning vacuum grease). The slit served as a flow chamber for the cells when a perfusate was infused from an open end of the slit and the effluent from the other end blotted with a paper wick. A semicircular plastic ring was glued to the proximal end of the perfusion slit to serve as a miniperfusate container into which perfusate was continuously added via a pipette connected to a Harvard syringe pump. The chamber was mounted on a thermostated stage (at 30°C) of an Olympus BH upright microscope. In order to coat the cover glass with poly-L-lysine (M_r 10–40K, Sigma), 5 μl of a 1 mg/ml H_2O solution was placed in the marked center of the cover glass and allowed to dry. The slide was washed for 5 to 10 sec with running deionized distilled water and air dried. A 2–3 μl aliquot of cell suspension was placed on the polylysine-coated surface and allowed to adhere for 30 sec. The cover glass was inverted (with cells on its lower surface), placed on the slide glass with a slit-like perfusion groove, sealed with silicone grease, and further secured with dental wax. When Ringer's solution was infused into the slit with a perfusion pipette connected to an infusion pump, unattached cells were lost. Polylysine coating was adjusted (by changing the duration of washing) so that a sufficient number of cells were loosely attached to the cover glass. Since removal of HCO_3 had no effect on MCh-induced cell shrinkage (*see* the Table), HCO_3-free HEPES-Ringer's solution was used unless otherwise noted. The HEPES-Ringer's solution contained (in mM): 144.2 NaCl, 5 KCl, 1.2 $MgSO_4$, 1.0 $CaCl_2$, 1.2 NaH_2PO_4, 10 HEPES acid/NaHEPES (where [Na] was usually 5.8 mM), 5.5 glucose, 20 mg/100 ml bovine serum albumin (BSA), at pH 7.48 and gassed with air or O_2. The microscope/video system consisted of a 100× oil-immersion objective, a DIC condenser system (1.25×), a 15× photomicrograph eyepiece, and a Panasonic (Secaucas, NJ) WV-1850 high-resolution neuvicon CCTV camera (8×). Thus the total magnification was 15,000×. Focus was frequently adjusted so as to obtain the maximal diameter of the cell. In preliminary experiments, we confirmed that the decrease of the cell diameter in the horizontal direction is comparable to that in the vertical direction when the vertical diameter of the cell was determined by optical cross sectioning (the decrease of the vertical diameter during 3 μM MCh-induced cell shrinkage was 12 ± 0.7% (mean ± SE) and that of the horizontal diameter 11.5 ± 0.3%, $P > 0.1$, $n = 5$). The video image was recorded with a Panasonic NV-8950 VCR equipped with a WJ-810 time-date generator. The maximal cross section of the cell was determined by manually tracing the border of the cell in a still frame and using an area determination program (Digital Paint Brush System, Jandel Scientific, Corte Madera, CA). For each frame, the tracing was repeated three or four times and its mean was used for calculation of the cell volume, assuming that the cell was a perfect sphere (*see* Appendix). The variation in the values of the traced cell area in each still frame was less than 2%. In a preliminary experiment, an attempt was made to export the video image to a graphic program (such as Canvas, Deneva Software, Miami, FL), using an appropriate image grabber for a Macintosh IIx computer, and the captured image traced with a pointer and analyzed. Although the accuracy of the two methods was comparable, the latter method was more time consuming. All the reagents were obtained from Sigma (St. Louis, MO) unless otherwise noted. Quinidine, W-7, ionomycin, and DPC were dissolved in 10 or 100 mM stock solutions of DMSO and added to the medium to make the final drug concentrations. The final concentration of DMSO in the medium never exceeded 1 mM. DMSO (1 mM)

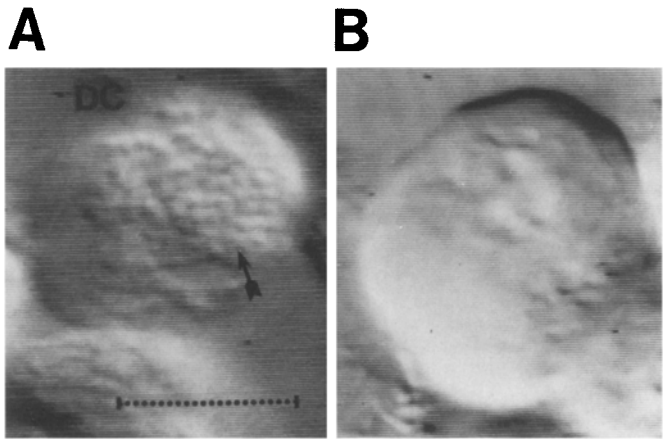

Fig. 1. Examples of (*A*) a dark cell and (*B*) a myoepithelial cell as shown on a video monitor. Note that the dark cell is readily identified by the presence of uniformly sized dark cell granules (arrow in *A*), especially clear during optical sectioning with DIC. In contrast, the myoepithelial cell (*B*) is larger and filled with dense amorphous cytoplasmic masses (presumably myofilaments) containing a smaller number of mitochondria-like granules. The interrupted bar indicates 10 μm

Table 1. Effects of Na-, K-, Cl-, and HCO_3-free HEPES buffer and 0.1 mM bumetanide on MCh-induced cell shrinkage of eccrine clear cells

Ringer's solution	*n*	% Cell volume during MCh stimulation	
		Control	Experimental
Na-free	5	79.0 ± 2.5[a]	77.6 ± 2.0
K-free	6	79.5 ± 2.1	80.8 ± 0.3
Cl-free	5	83.5 ± 2.1	83.0 ± 1.2
HCO_3-free	5	79.4 ± 3.2	78.0 ± 0.3
Bumetanide (0.1 mM)	5	81.0 ± 2.1	80.6 ± 0.1
Ouabain (0.1 mM)	4	74.5 ± 1.9	73.8 ± 1.3

[a] The data expressed as the mean ± SEM of the lowest % cell volume after MCh (3 μM) stimulation (i.e., 100% is the cell volume of prestimulation period). In all cases, the differences between control and experimental were not statistically significant ($P > 0.1$). HCO_3 was removed from HEPES bicarbonate buffer (which is similar to KRB except 10 mM HEPES was added to stabilize pH), whereas other ions were removed from (HCO_3-free) HEPES-Ringer's solution. The cells had been equilibrated with experimental solutions for 1 min before MCh (in the same solutions) was added. HEPES-Ringer's solution was used for bumetanide experiments. *n*, number of cells studied.

alone had no effect on cell volume or on the effect of MCh (*data not shown*).

Results

Figure 2 shows representative video images of a dissociated clear cell in the resting state (Fig. 2*A*, continuously perfused with HEPES-Ringer), after stimulation with 3 μM MCh for 20 sec (Fig. 2*B*), and after the subsequent wash out of MCh with HEPES-Ringer (Fig. 2*C*). Note the change in cell size (Fig. 2*B*) relative to the 12-μm long bar placed on the video monitor. MCh-induced cell shrinkage occurs within a few seconds of exposure to MCh if a high perfusion rate is employed. However, in order to avoid the detachment of cells from the cover glass, we had to use a low infusion rate of 50–100 μl per min. Under this condition, 10 sec was needed for the MCh solution to flow through the slit and reach the cell, which was subtracted from the actual time of solution change. In about two-thirds of the cells (more than 60 cells counted), the cell size gradually recovered to 80 to 90% of the prestimulation level within 5–10 min of continuous stimulation with 3 μM MCh (Fig. 3*A*). About a third of the cells, however, remained shrunken without cell volume increase for as long as 5–10 min of stimulation (Fig. 3*B*). After removal of MCh, the cells immediately began swelling to reach the prestimulation level, but some cells showed varying degrees of transient rebound swelling during the wash out period (Fig. 3*A*). Three cells showed an oscillation pattern similar to that reported in the parotid acinar cells (Foskett & Melvin, 1989). As shown in Fig. 4, MCh-induced maximal cell shrinkage was dose dependent, plateauing at around 3 μM. However, at low MCh concentrations, e.g., 0.01 μM, the initial cell shrinkage was followed by complete volume recovery to the resting level during stimulation (Fig. 5*A*) and only one of 10 cells showed a persistent shrinkage pattern (Fig. 5*B*). The observed MCh-induced cell shrinkage is pharmacologically specific because the effect of 3 μM MCh is completely inhibited by 10 μM atropine ($n = 5$, *not shown*).

We then set out to examine the thesis that the MCh-induced cell shrinkage is due to activation of K and Cl channels by cholinergic stimulation, resulting in the net efflux of cytoplasmic KCl from the cell and cell shrinkage. First, as shown in the Table, the effect of external ions, ouabain, and bumetanide

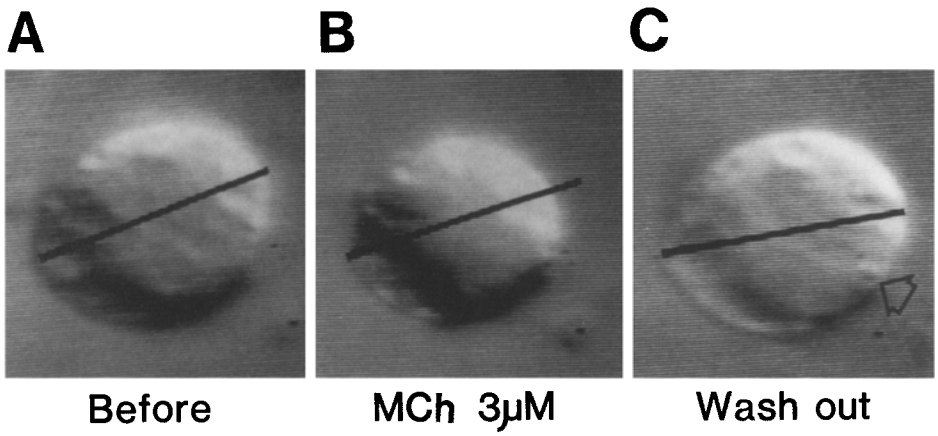

Fig. 2. Example of a clear cell (*A*) before stimulation, (*B*) cell shrinkage in response to 3 μM MCh stimulation, and (*C*) the recovery after washout of the drug. In this illustrative experiment, the cell is focused so that the largest diameter can be optically sectioned by DIC optics. The tape, proportional to 12 μm, was pasted over the cell on the monitor for photographing. The clear cell is easily identified by the presence of characteristic lipofuscin granules (arrow in *C*), by the presence of abundant small cytoplasmic granules (presumably mitochondria), and by the exclusion of other cell types

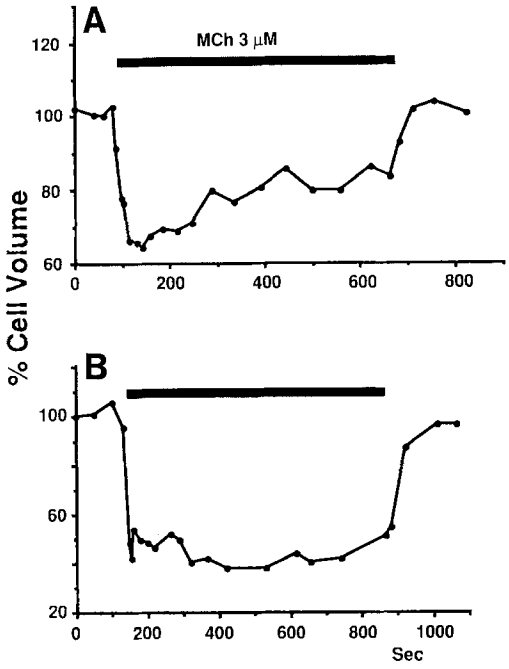

Fig. 3. The two most frequent time courses of 3 μM MCh-induced cell shrinkage. (*A*) Most clear cells showed a biphasic pattern showing the initial maximal shrinkage followed by gradual recovery of cell volume to 80 to 90% of the resting cell volume. (*B*) In about a third of cells, however, MCh-induced cell shrinkage was more persistent. Throughout the study, the minimal cell volume (and thus the maximal MCh-induced cell shrinkage) was expressed relative to the resting cell volume, usually that at time 0. There was no convincing difference in the degree of cell shrinkage between the cells that recovered and those that did not, i.e., 32.2 ± 1.9 (n = 40) for the former and 31.6 ± 3.8 (n = 12) for the latter, $P > 0.1$

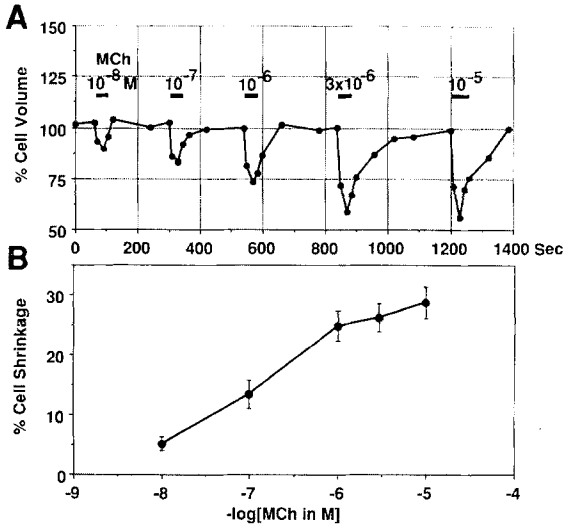

Fig. 4. MCh dose *versus* maximal cell shrinkage. (*A*) An illustrative example of a dose-response study where different MCh concentrations were applied in pulses to determine the magnitude of the maximal cell shrinkage. (*B*) Each plot is the mean ± SEM of 16 to 38 cells

on MCh-induced cell shrinkage was studied. The lack of inhibition by ouabain or bumetanide of MCh-induced cell shrinkage suggests that a Na pump or bumetanide-sensitive Na-K-2Cl cotransporters may not be directly involved. Furthermore, the lack of effects upon removal of external Na, Cl, HCO_3 and K on MCh-induced cell shrinking is also consistent with the notion that a Na-K exchange pump (which requires external K) or parallel Na/H and Cl/HCO_3 exchangers (Geck & Heinz, 1986; O'Grady, Palfrey & Field, 1987) may not be directly involved in the

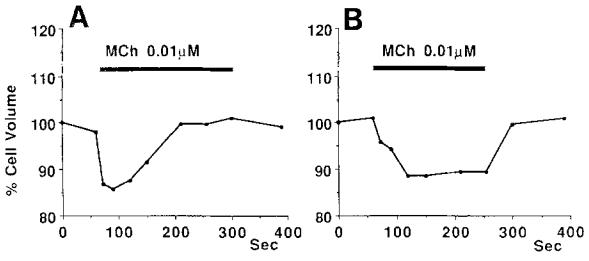

Fig. 5. Time course of cell shrinkage induced by 0.01 μM MCh. Nine of 10 cells showed a spontaneous recovery of cell volume in the continuous presence of MCh as in (*A*) (a single illustrative example), whereas only one cell showed the persistent shrinkage (*B*)

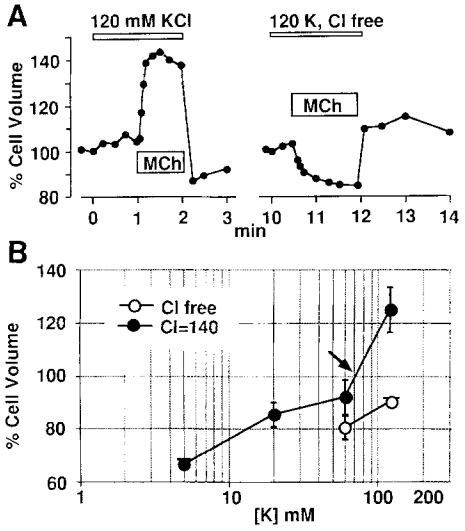

Fig. 6. Effect of extracellular K and Cl concentrations on MCh-induced cell shrinkage. (*A*) Left trace is an illustrative experiment where the medium [K] was increased from 5 to 120 mM at the expense of Na during the period indicated by the bar. Cl concentration (157 mM) was unchanged. Note the cell swelling in response to 3 μM MCh. The right trace shows the same cell shrinking in response to MCh after Cl was replaced by gluconate while [K] was kept at 120 mM. (*B*) MCh-induced change in cell volume in different external [K] and [Cl]. The arrow in *B* indicates $[K]_o$ where MCh-induced cell shrinkage was nullified, i.e., the experimentally obtained $[K]_{o,null}$. Each plot is the mean ± SEM of six to eight cells

MCh-induced cell shrinkage either. Second, the effect of the chemical potential gradient on MCh-induced cell shrinkage was studied because KCl movement via KCl cotransporters or K and Cl channels would be reversed if the combined K and Cl chemical potential gradient outside the cell was made larger than that inside the cell (i.e., $[K]_o \cdot [Cl]_o > [K]_i \cdot [Cl]_i$). Indeed, as shown in Fig. 6, when the external K was increased to 120 mM (at the expense of Na, with $[Cl]_o$ unchanged at 157 mM), stimulation with MCh caused cell swelling (Fig. 6*A*, left trace)

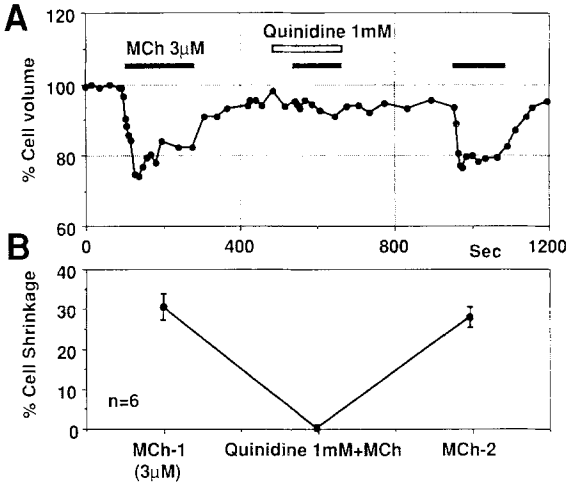

Fig. 7. Inhibition of MCh-induced cell shrinkage by quinidine. (*A*) An illustrative experiment. (*B*) The summary of six similar studies. Each plot is the mean ± SEM

because $[K]_o \cdot [Cl]_o$ (= 120 × 157) was larger than $[K]_i \cdot [Cl]_i$ (= 125 × 90) (Takemura et al., 1991). As shown in the right trace in Fig. 6*A*, MCh-induced cell shrinking was partially restored when $[Cl]_o$ was reduced to zero by replacing Cl_o with a less permeable anion, gluconate (while keeping $[K]_o$ at 120 mM), because then $[K]_o \cdot [Cl]_o$ was definitely smaller than $[K]_i \cdot [Cl]_i$. Furthermore, at the theoretical null, $[K]_o$ ($[K]_{o,null}$ where the cell volume does not change during MCh stimulation because $[K]_{o,null} \cdot [Cl]_o = [K]_i \cdot [Cl]_i$) should be consistent with the experimentally derived value. In fact, the predicted $[K]_{o,null}$ of 71.7 mM (calculated from $[K]_i \cdot [Cl]_i/[Cl]_o$ = (125 × 90)/157) agrees with the experimentally obtained value of 71 mM (the intercept of the cell shrinkage curve with the 100% line indicated by the arrow in Fig. 6*B*). In order to further substantiate the thesis that MCh-induced KCl efflux is mediated by K and Cl channels rather than by KCl cotransporters (Corcia & Armstrong, 1983; Reuss, 1983), the effects of putative K and Cl blockers, quinidine and DPC, respectively, were studied. As shown in Fig. 7, quinidine at 1 mM completely inhibited MCh-induced cell shrinkage, but removal quinidine restored the cell's responsiveness to MCh. Another commonly used blocker of K channels, barium (Ba) at 5 mM, also inhibited MCh-induced cell shrinkage, although to a lesser extent (29.4 ± 3.3% (mean ± SE) of cell shrinkage by 3 μM MCh was reduced to 9.1 ± 4.8% by Ba + MCh, $n = 7$, $P < 0.002$; the post-experimental MCh-induced shrinkage was 25.6 ± 3.4%). The putative blocker of Cl-channels, DPC at 1 mM (Gögelein, 1988), also partially inhibited MCh-induced cell shrinkage in a reversible fashion (*see* Fig. 8; note that DPC could also inhibit Cl^-/HCO_3^- exchangers; Reuss, Constantin & Bazile, 1987), although the in-

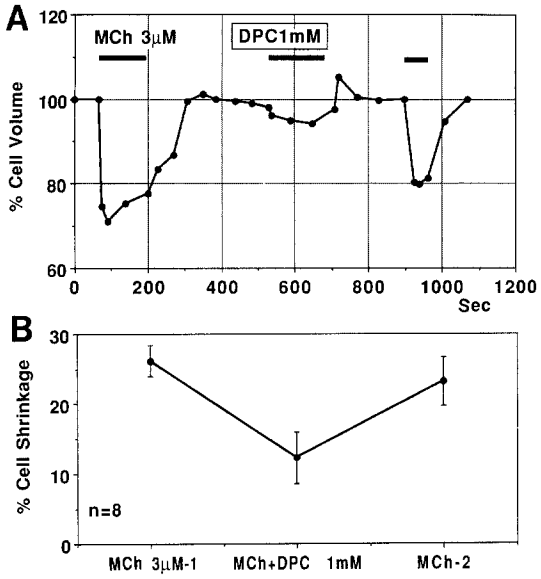

Fig. 8. Partial inhibition of MCh-induced cell shrinkage by DPC. (*A*) An illustrative experiment. (*B*) The summary of eight similar experiments. Each plot is the mean ± SEM. *P* (the significance by the Student's *t* test) < 0.01; *n*, the number of cells studied

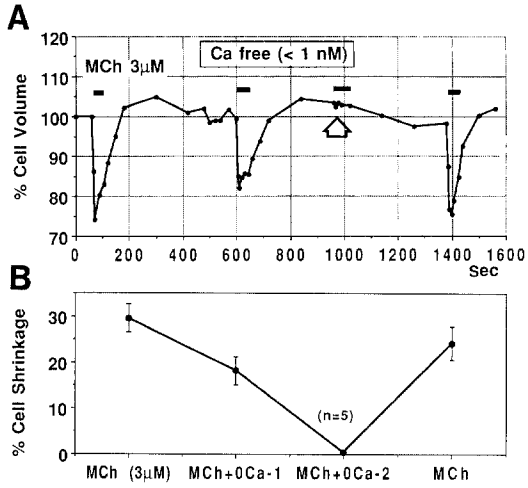

Fig. 9. Effect of Ca-free medium on MCh-induced cell shrinkage. (*A*) An illustrative experiment. Note that the first MCh stimulation in the Ca-free (also containing 1 mM EGTA) medium induced considerable cell shrinkage, whereas the second MCh stimulation had no effect (arrow). MCh responsiveness was fully reversible on readmission of Ca. (*B*) Depicts the means ± SEM of five similar experiments

hibitory effect of DPC was variable in different cells. Since observations obtained thus far supported the involvement of K and Cl channels as the mechanism of MCh-induced cell shrinkage, we then studied the role of intracellular Ca in regulation of the channel activity. We previously had observed that cytoplasmic free [Ca] increased several-fold during stimulation with MCh (Sato & Sato, 1988), so we initially expected that reduction of extracellular Ca below the nanomolar range (Ca-free Ringer containing 1 mM EGTA) should drastically inhibit MCh-induced cell shrinkage. However, the cells did partially respond to MCh once, even in the Ca-free medium (*see* Fig. 9). Interestingly, the same cell no longer responded to the second MCh exposure (arrow in Fig. 9*A*) in the same Ca-free medium, suggesting that the cell shrinkage after the first MCh stimulation in the Ca-free medium was most likely due to mobilization of Ca from the endogenous stores and that the endogenous Ca stores were quickly depleted by a single stimulation with MCh. The importance of Ca is further suggested because the Ca ionophore, ionomycin, also caused cell shrinkage in a dose-dependent fashion (Fig. 10). However, 10 μM ionomycin, which induced the same magnitude of cell shrinkage as 3 μM MCh, tended to damage cells as suggested by the appearance of blebbing. Since calmodulin is often implicated in Ca-mediated activation of K and Cl channels (Lewis & Donaldson, 1990), we also studied the effect of a putative calmodulin inhibitor, W-7 (Hidaka & Tanaka, 1983).

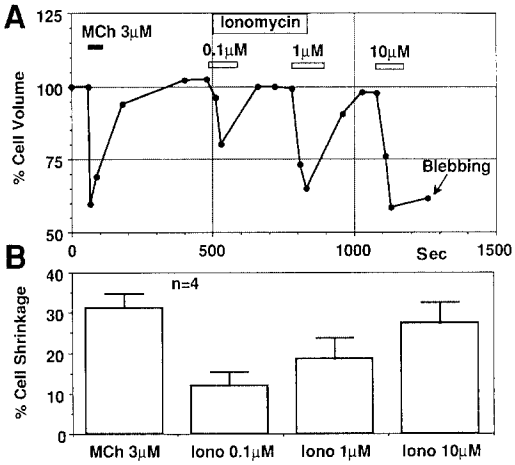

Fig. 10. Ionomycin-induced cell shrinkage. (*A*) An illustrative experiment. (*B*) The means ± SEM of four similar experiments. The medium used is the same as in other experiments (i.e., HEPES-Ringer containing Ca)

As shown in Fig. 11, W-7 drastically inhibited the effect of MCh on cell shrinkage, with the recovery of MCh responsiveness after W-7 treatment was removed. That the inhibitory effect of W-7 is not due to nonspecific inhibition of protein kinase C is suggested because a protein kinase inhibitor, 1-(5-isoquinolinesulfonyl)-2-methylpiperazine hydrochloride (H-7) (Conquer & Mahadevappa, 1990) at 0.1 mM, had no effect on MCh-induced cell shrinkage ($n = 5$, *data not shown*).

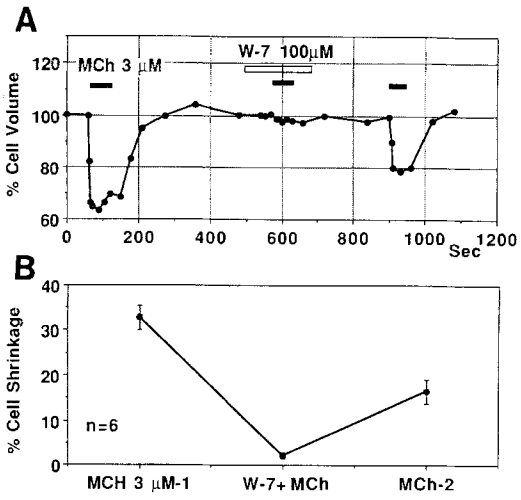

Fig. 11. Inhibition of MCh-induced cell shrinkage by 0.1 mM W-7. (*A*) An illustrative experiment. (*B*) The means ± SEM of six similar experiments

Discussion

We have recently reported that cholinergic stimulation of the eccrine clear cell is associated with significant cell volume decrease (Saga & Sato, 1989; Takemura et al., 1991). The main aim of the present study was therefore to elucidate the mechanism by which cholinergic stimulation results in cell volume decrease of as much as 30% of resting cell volume. Elucidation of its mechanism would further our understanding of the ionic mechanism of eccrine sweat secretion in health and disease.

In the present study, we observed: (*i*) the microscopic video images provide sufficient resolution for identifying different cell types and for determining the volume of a single cell; (*ii*) MCh shrinks clear cells in a dose-dependent, reversible, and pharmacologically specific fashion; (*iii*) MCh-induced cell shrinkage is monophasic (or persistent) in some cells and biphasic (with the initial maximal cell shrinkage followed by varying recovery of cell volume) in others (such a recovery is more marked at low MCh concentrations); (*iv*) the MCh-induced cell volume change is dependent on the combined chemical potential gradients for K and Cl so that by reversing the gradient by increasing extracellular [K] to 120 mM, MCh now induces cell swelling; (*v*) the null concentration of K at which cell volume does not change by MCh exposure ($[K]_{o,null}$) which was determined experimentally agrees closely with the value estimated using the reported intracellular [K] and [Cl] (Takemura et al., 1991); (*vi*) MCh-induced cell shrinkage is completely inhibited by quinidine, an inhibitor of Ca-dependent K channels; (*vii*) a putative inhibitor of Cl channels, DPC, partially blocks MCh-induced cell swelling; (*viii*) in the absence of Ca in the bath, the clear cell responds to MCh only once and fails to respond after the second MCh dose; (*ix*) introduction of Ca into the cell by ionomycin also induces cell shrinkage in a dose-dependent manner; (*x*) a putative inhibitor of calmodulin, W-7, completely inhibits MCh-induced cell shrinkage in a partially reversible manner; (*xi*) MCh-induced cell shrinkage is not affected by removal of Na, K, Cl, or HCO_3 from the bath; and (*xii*) neither bumetanide nor ouabain inhibited MCh-induced cell shrinkage.

We previously reported that cholinergic stimulation is associated with K efflux from the sweat secretory coils (Saga, Sato & Sato, 1988) and the decrease of intracellular [Cl] and [K] (Saga & Sato, 1989; Takemura et al., 1991). Thus, the present data further substantiate the thesis that the cell shrinkage associated with cholinergic stimulation is caused by the efflux of KCl. Similar cholinergic stimulation of KCl efflux (Cook & Young, 1989) and cell shrinkage (Foskett & Melvin, 1989; Nakahari et al., 1990) have been reported in salivary glands. However, the mechanism whereby MCh causes the net KCl efflux and cell shrinkage, as well as its functional significance, is still poorly understood. Ion channels, including K and Cl channels, are ubiquitously present in nonepithelial as well as epithelial cells, including the salivary acinar cells (Gögelein, 1988; Cook & Young, 1989) and eccrine clear cells (Sato & Sato, 1989). It is well established that K and Cl channels are essential components in the Na-K-2Cl cotransport model (Geck & Heinz, 1986; O'Grady et al., 1987). Evidence is increasing that such a cotransport mechanism is also involved in the ion transport of salivary and eccrine acini (Cook & Young, 1989; Sato et al., 1989). Nevertheless, the Na-K-2Cl cotransport model itself does not require the net outflux of KCl or the subsequent dramatic cell volume decrease, i.e., K is assumed to simply recycle across the basolateral membrane via K channels, Na/K exchange pumps, and Na-K-2Cl cotransporters.

The other salient situation where the net KCl efflux from the cell plays a significant role occurs during regulatory volume decrease (RVD), an attempt by the cell to restore the original cell volume following cell swelling in hypotonic media (Chamberlin & Strange 1989; Lewis & Donaldson, 1990). The strategies that cells employ for achieving the net KCl loss during RVD vary in different cell types but they include Ca-dependent K and Cl channels, electroneutral KCl cotransporters, a Na-Ca exchanger coupled with Ca efflux via Ca-ATPase, or parallel K-H and Cl-HCO_3 exchangers. Although MCh-induced cell shrinkage in the eccrine clear cell is apparently distinct from RVD in that the MCh-

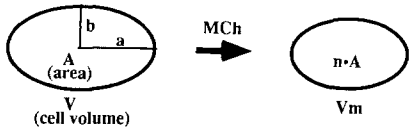

Fig. 12. An ellipsoid with a long axis of $2a$ and a short axis of $2b$ (created by revolution of the ellipse about the horizontal axis). After stimulation with MCh, the cross-sectional area changed from A to $n \cdot A$ and the cell volume from V to V_m

induced shrinkage is the primary cellular response to MCh *versus* the secondary corrective response of the cell to osmotic cell swelling in RVD, the two cellular responses may share the same transport processes and may be mediated by the increase in cytoplasmic Ca (Chamberlin & Strange, 1989; Lewis & Donaldson, 1990). In MCh-induced cell shrinkage, removal of external Na, Cl, K, or HCO_3 had no significant effect, suggesting that Na-Ca exchange or parallel K-H and Cl-HCO_3 exchangers may not be directly involved as its mechanism. Both KCl cotransporters and K and Cl channels depend on the chemical potential gradients to facilitate KCl movement. However, inhibition of MCh-induced cell shrinkage by quinidine (K channel blocker) and DPC (Cl channel blocker), its dependence on cytoplasmic Ca, and its inhibition by W-7 (putative calmodulin inhibitor) are all supportive of the notion that MCh-stimulated KCl movement (and thus cell shrinkage) is mediated by Ca-dependent activation of K and Cl channels because the KCl cotransporters are not known to respond to these experimental manipulations. In view of the indirect nature of our observations, the present conclusion is still tentative.

Nevertheless, the occurrence of the dramatic cell shrinkage during cholinergic stimulation is undeniable. A number of questions remain unanswered. Cl conductance also appears to be present in the basolateral membrane (Sato, 1986), so where are the Cl channels that are involved in the net KCl efflux located? Why is cell shrinkage important in terms of stimulating sweat secretion? Are Cl and K channels both activated by Ca or is only one of these channels regulated while the other is left open at rest? What is the ultimate mechanism of channel regulation by Ca? Can the method be made more sensitive in order to study the regulation of ion channels in defective cells such as cystic fibrosis cells or mutated cells? Since the determination of cell volume change during various experimental manipulations is relatively less invasive to the cell than other available methods, such as patch clamping, it will continue to be useful in further understanding the regulation of membrane transport in epithelial cells.

This paper has been supported in part by NIH grants DK 27857 and AR 25339 and Cystic Fibrosis Foundation Grant G124. Sue Cavallin helped in preparation of the manuscript.

References

Chamberlin, M.E., Strange, K. 1989. Anisosmotic cell volume regulation: A comparative view. *Am. J. Physiol.* **257:**C159–C173

Conquer, J., Mahadevappa., V.G. 1990. Inhibition of protein kinase C by H-7 potentiates the release of oleic, linoleic and arachidonic acids in A23187-stimulated human neutrophils. *Biochem. Biophys. Res. Commun.* **167:**168–173

Cook, D.I., Young, J.A. 1989. Fluid and electrolyte secretion by salivary glands. *In:* Handbook of Physiology. The Gastrointestinal System III. S.G. Schultz and J.G. Forte, editors, pp 1–23. American Physiological Society, Bethesda (MD)

Corcia, A., Armstrong, W.M. 1983. KCl cotransport: A mechanism for basolateral chloride exit in *Necturus* gallbladder. *J. Membrane Biol.* **76:**173–182

Foskett, J.K., Melvin, J.E. 1989. Activation of salivary secretion: Coupling of cell volume and $[Ca^{2+}]_i$ in single cells. *Science* **24:**1582–1585

Geck, P., Heinz, E. 1986. The Na-K-2Cl cotransport system. *J. Membrane Biol.* **91:**97–105

Gögelein, H. 1988. Chloride channels in epithelia. *Biochim. Biophys. Acta* **947:**521–547

Hidaka, H., Tanaka, T. 1983. Naphthalenesulfonamides as calmodulin antagonists. *Methods Enzymol.* **102:**185–194

Izutsu, K., Johnson, D.E. 1986. Changes in elemental concentrations of rat parotid acinar cells following pilocarpine stimulation. *J. Physiol.* **381:**297–309

Lewis, S.A., Donaldson, P. 1990. Ion channels and cell volume regulation: Chaos in an organized system. *News Physiol. Sci.* **5:**112–119

Nakahari, T., Murakami, M., Yoshida, H., Miyamoto, M., Sohma, Y., Imai, Y. 1990. Decrease in rat submandibular acinar cell volume during ACh stimulation. *Am. J. Physiol.* **258:**G878–G886

O'Grady, S.M., Palfrey, H.C., Field, M. 1987. Characteristics and functions of Na-K-Cl cotransport in epithelial tissues. *Am. J. Physiol.* **253:**C177–C192

Reuss, L. 1983. Basolateral KCl cotransport in a NaCl-absorbing epithelium. *Nature* **305:**723–726

Reuss, L., Constantin, J.L., Bazile, J.E. 1987. Diphenylamine-2-carboxylate blocks $Cl^-HCO_3^-$ exchange in *Necturus* gallbladder epithelium. *Am. J. Physiol.* **253:**C79–C89

Saga, K., Sato, K. 1989. Electron probe X-ray microanalysis of cellular ions in the eccrine secretory coil cells during methacholine stimulation. *J. Membrane Biol.* **107:**13–24

Saga, K., Sato, K., Sato, F. 1988. K^+ efflux from monkey eccrine secretory coil during the transient stimulation with agonists. *J. Physiol.* **405:**205–217

Sasaki, S., Nakagaki, I., Mori, H., Imai, Y. 1983. Intracellular calcium store and transport of elements in acinar cells of the salivary gland determined by electron probe x-ray microanalysis. *Jpn. J. Physiol.* **33:**69–83

Sato, K. 1986. Effect of methacholine on ionic permeability of basal membrane of the eccrine secretory cell. *Pfluegers Arch.* **407 (Suppl. 2):**S100–S106

Sato, K., Kang, H.W., Saga, K., Sato, K.T. 1989. Biology of the eccrine sweat gland. I: Mechanism of sweat secretion. *J. Am. Acad. Dermatol.* **20:**537–565

Sato, K., Sato, F. 1981. Pharmacologic responsiveness of isolated single eccrine sweat glands. *Am. J. Physiol.* **240:**R44–R51

Sato, K., Sato, F. 1988. Relationship between Quin 2-determined cytosolic [Ca^{2+}] and sweat secretion. *Am. J. Physiol.* **254:**C310–C317

Sato, K., Sato, F. 1989. Characteristics of Na, K, and Cl channels in the clear cell membrane of the eccrine sweat gland as studied by the patch clamp techniques. *Clin. Res.* **37:**369A

Takemura, T., Sato, F., Saga, K. Suzuki, Y., Sato, K. 1991. Intracellular ion concentrations and cell volume during cholinergic stimulation of eccrine secretory coil cells. *J. Membrane Biol.* **119:**211–219

Received 2 October 1990; revised 5 February 1991

Appendix

In order to determine the change in relative cell volume, we assumed that the cell is a perfect sphere with a radius r, the maximal cross-sectional area A, and the volume V. Then

$$a = b = r,\ A = \pi r^2,\ V = (4\pi/3) \cdot r^3 = (4\pi/3) \cdot (A/\pi)^{\frac{3}{2}}. \quad \text{(A1)}$$

After MCh stimulation, A changed to $n \cdot A$, V to V_m, where n is a factor. The relative cell volume $= (V_m/V) = n^{\frac{3}{2}}$ [e.g., if $n = 0.8$, $(V_m/V) = 0.716$]. However, if the cell is an ellipsoid as in Fig. 12, and when $a = yb$ where y is a variable determined by the cell shape:

$$A = \pi ab = y\pi b^2,\ V = (4\pi/3)ab^2 = (4y\pi/3) \cdot (A/y\pi)^{\frac{3}{2}},$$

$$\text{and } b = (A/y\pi)^{\frac{1}{2}}. \quad \text{(A2)}$$

After MCh stimulation, the cross-sectional area of the cell reduced to $n \cdot A$. We also assume that the cell shrinks in both directions to the same extent, not an unreasonable assumption. Then

$$V_m = (4y\pi/3) \cdot (A/y\pi)^{\frac{3}{2}} \cdot n^{\frac{3}{2}}, \text{ and } (V_m/V) = n^{\frac{3}{2}}. \quad \text{(A3)}$$

Thus, the change in the maximal cross-sectional area of the cell as determined in the present study reflects the relative cell volume relatively independently of the cell shape.